PERGAMON International Journal of Mechanical Sciences 43 (2001) 487–504

International Journal of MECHANICAL SCIENCES

www.elsevier.com/locate/ijmecsci

Effect of inclusions and holes on the stiffness and strength of honeycombs

C. Chen, T.J. Lu, N.A. Fleck*

Department of Engineering, Cambridge University, Trumpington Street, Cambridge CB2 1PZ, UK

Received 30 June 1999; received in revised form 25 October 1999

Abstract

A finite element study has been performed on the effects of holes and rigid inclusions on the elastic modulus and yield strength of regular honeycombs under biaxial loading. The focus is on honeycombs that have already been weakened by a small degree of geometrical imperfection, such as a random distribution of fractured cell walls, as these imperfect honeycombs resemble commercially available metallic foams. Hashin–Shtrikman lower and upper bounds and self-consistent estimates of elastic moduli are derived to provide reference solutions to the finite element calculations. It is found that the strength of an imperfect honeycomb is relatively insensitive to the presence of holes and inclusions, consistent with recent experimental observations on commercial aluminium alloy foams.

Keywords: Honeycombs; Imperfections; FEM; Hashin-Shtrikman bounds; Self-consistant method

1. Introduction

Metallic foams show much potential for use in light-weight components of transportation vehicles, for example as the core of sandwich panels. Compared to conventional light-weight materials such as aluminium honeycombs and polymeric foams, current commercially available metallic foams possess a large number of processing-induced geometrical imperfections that degrade the foam properties. A review of these defects and their influence on the elastic and plastic properties of honeycombs can be found in Chen et al. [1]. Specifically, it is found that fractured cell walls produce the largest knock-down effect in yield strength of honeycombs, followed in order by

* Corresponding author. Tel.: + 44-01223-332650; fax: + 44-01223-332662.
E-mail address: naf1@eng.cam.ac.uk (N.A. Fleck).

0020-7403/01/$ - see front matter
PII: S0020-7403(99)00122-8

missing cells, cell-wall waviness, cell-wall misalignment, cell-size variations and non-uniform cell-wall thickness. It is further established that a small degree of morphological imperfection suffices to induce cell-wall bending, reducing the hydrostatic yield strength to the same level as that of the uniaxial yield strength. The recent yield surface measurements by Deshpande and Fleck [2] show that the hydrostatic and deviatoric strengths of metallic foams are, in fact, comparable.

The focus of the present study is the knock-down in stiffness and strength due to redundancy defects in the form of rigid inclusions, and vacancy defects in the form of holes, within an initially perfect or imperfect honeycomb. An imperfect honeycomb is created by introducing a random distribution of a small number of fractured cell walls in a perfect hexagonal honeycomb. Finite element predictions are given for the uniaxial and hydrostatic properties; the predicted elastic moduli are compared with those provided by the Hashin–Shtrikman lower and upper bounds, and by self-consistent estimates. In a closely related previous study, Guo and Gibson [3] used the finite element method to study the effect of holes on the elasto-plastic behaviours of perfect honeycombs subjected to uniaxial loading. The present investigation builds upon that of Guo and Gibson [3] as follows: (a) the effects of both rigid inclusions and holes are studied; (b) periodic boundary conditions rather than frictionless grips boundary conditions are implemented; (c) both perfect and imperfect honeycombs are considered; and (d) the mechanisms underlying the significant knock-down of stiffness and strength under hydrostatic loading are explored.

2. Finite element models

Following Chen et al. [1] and other related studies [3,4], regular hexagonal honeycombs are selected as the fundamental geometry for modelling metallic foams. Prior to the introduction of holes or inclusions, the underlying honeycomb structure is taken to be either perfect or imperfect. The imperfect honeycomb has 5% of its cell walls randomly removed, as shown in Fig. 1a; the arrows denote the fractured cell walls. This level of imperfection, although unrealistically large for practical honeycombs, enables the honeycomb to simulate the observed multi-axial yield response of a 3D foam, as discussed by Chen et al. [1] and Deshpande and Fleck [2]. It is known that the in-plane elastic properties of perfect hexagonal honeycombs are isotropic whilst their plastic properties are almost isotropic [1,5,6]. The elasto-plastic behaviour of a honeycomb containing a random distribution of defects may also be assumed to be isotropic.

Fig. 1b presents the finite element mesh for an imperfect honeycomb containing a rigid inclusion or a traction-free hole. Here, 19 hexagonal cells are occupied by both the inclusion and the hole, but this number will be varied later to study the size effect. Furthermore, the inclusions and holes considered are only approximately circular in shape due to the hexagonal cellular structure of the honeycomb. The finite element model assumes that the domain bounded by ABCDA in Fig. 1b represents a periodic unit cell, of size $L \times L$, representative of an infinitely large honeycomb. Each cell wall is modelled by six quadratic Timoshenko beam elements (the B22 element in the finite element code ABAQUS); in earlier work Chen et al. [1] have demonstrated that the use of six B22 elements for each cell wall leads to satisfactory predictions of the response for regular honeycombs having low relative densities (< 0.3). The cell-wall material is taken as elastic–perfectly-plastic with Young's modulus $E_s = 69$ GPa and yield strength $\sigma_y = 130$ MPa, typical of aluminium alloys, giving $\sigma_y/E_s = 0.00188$. To simplify mesh generation, the rigid inclusion is ascribed the

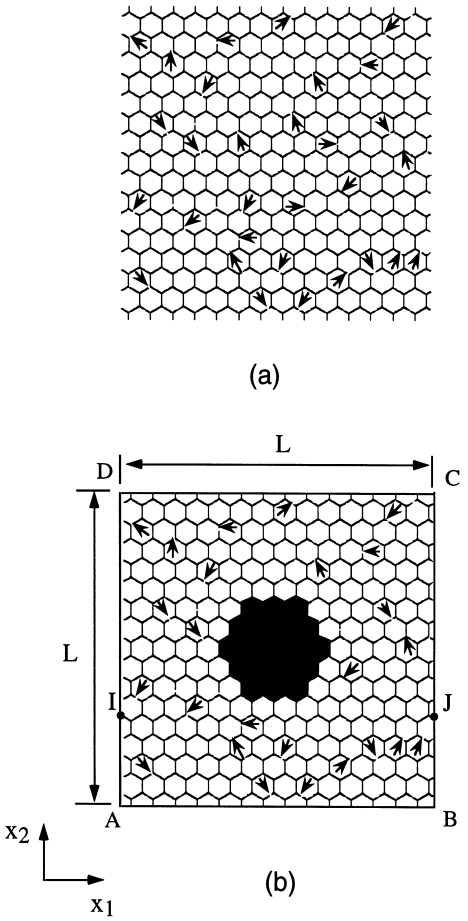

Fig. 1. Finite element mesh of an imperfect honeycomb with (a) no inclusion or hole, (b) a rigid inclusion or a circular hole, shown by the blackened region of the mesh. The small arrows denote the locations of broken cell walls.

microstructure of a perfect honeycomb, but Young's modulus and yield strength of the cell-wall material are 1000 times those of cell-wall material outside the inclusion.

The effect of the presence of inclusions or holes on the elastic and plastic properties of honeycombs is parameterised in terms of the length scale D, where

$$D = 3^{1/4}\sqrt{\frac{6}{\pi}Nl}. \tag{1}$$

Here, N is the number of hexagonal cells occupied by the inclusion (or hole) and l is the cell-wall length. Thus, D equals the diameter of an imaginary circle, the area of which equals that of the inclusion (or hole). The volume fraction c of inclusion (or hole) in the unit cell is

$$c = \frac{\pi}{4}\left(\frac{D}{L}\right)^2, \tag{2}$$

where L is the side length of the unit cell.

It is important to ensure that appropriate boundary conditions are applied to the finite element mesh. As a rule, the selected boundary conditions should lead to the global behaviour of the honeycomb, and not to localised deformation near the boundaries of the mesh. We shall be guided in our choice of boundary conditions by the results of a previous study [1], and we review the previous findings briefly here. Three types of boundary conditions were considered by Chen et al. [1], namely, frictionless grips, sticking grips, and periodic boundary conditions. The frictionless grips boundary condition is enforced by prescribing the normal displacement along each boundary edge of the mesh, with vanishing tangential force and bending moment at each boundary node. The sticking grips boundary condition requires that the translation displacements u_α^J and rotation θ^J of every node on the boundary ABCDA in Fig. 1b satisfy

$$u_\alpha^J = \varepsilon_{\alpha\beta} x_\beta^J, \quad \theta^J = 0, \quad \alpha, \beta = 1, 2, \tag{3}$$

where $\varepsilon_{\alpha\beta}$ is the average macroscopic strain, x_β^J are the co-ordinates of a representative node J on ABCDA, and the summation convention applies over repeated suffices. The periodic boundary condition on ABCDA implies

$$u_\alpha^J - u_\alpha^I = \varepsilon_{\alpha\beta}(x_\beta^J - x_\beta^I), \quad \theta^J - \theta^I = 0, \quad \alpha, \beta = 1, 2 \tag{4}$$

for pairs of nodes I and J on opposite boundary edges of the mesh, as shown for example by the solid circles in Fig. 1b. Chen et al. [1] demonstrate that, for perfect honeycombs, only the finite element predictions obtained with the periodic boundary conditions agree closely with the analytical results — for hydrostatic loading, the frictionless boundary condition leads to much lower strengths whereas the sticking grips boundary condition results in an overestimation of the hydrostatic strength. Thus, the finite element calculations reported in the current study are performed using the periodic boundary conditions as stated by Eq. (4). The macroscopic stress is computed from the reaction forces sustained by the boundary nodes. Since the macroscopic behaviours of both the perfect and imperfect honeycombs are assumed to be isotropic, the imposed macroscopic shear strain ε_{12} can be taken to be zero in the finite element calculations without loss of generality. Two types of external loading — uniaxial stressing and hydrostatic pressure — are of primary interest in the present study. For uniaxial stressing along, say, the x_1 direction (Fig. 1b), the macroscopic strain ε_{11} is incremented and the ratio $\varepsilon_{22}/\varepsilon_{11}$ is adjusted such that σ_{22} is maintained equal to zero. For hydrostatic loading, the ratio $\varepsilon_{11}/\varepsilon_{22}$ is changed during deformation to ensure that $\sigma_{11} = \sigma_{22}$ throughout the loading history.

3. Results

3.1. Honeycombs without rigid inclusions or holes

Before exploring the influence of rigid inclusions and holes on the elastic stiffness and yield strength of elastic–perfectly-plastic honeycombs, it is educational to review these mechanical properties for honeycombs without inclusions or holes. For the case of a perfect honeycomb, the macroscopic Young's modulus E_0, bulk modulus κ_0, uniaxial yield strength σ_U^0 and hydrostatic

strength σ_H^0 are given by [6]

$$\frac{E_0}{E_s} = 1.5\bar{\rho}^3, \quad \frac{\kappa_0}{E_s} = 0.25\bar{\rho},$$

$$\frac{\sigma_U^0}{\sigma_y} = 0.5\bar{\rho}^2, \quad \frac{\sigma_H^0}{\sigma_y} = 0.5\bar{\rho}, \tag{5}$$

where E_s and σ_y are Young's modulus and yield strength of the cell-wall material, respectively. The relative density $\bar{\rho}$ of the regular hexagonal honeycomb is related to the cell size l and uniform wall thickness t by

$$\bar{\rho} = \frac{2}{\sqrt{3}}\frac{t}{l}, \tag{6}$$

where $t \ll l$ is assumed. In the present finite element calculations, $\bar{\rho}$ is changed by varying t at fixed l. The finite element predictions for a perfect honeycomb, of the unit cell size $L \times L$ and subjected to periodic boundary conditions, agree well with Eq. (5). In addition, it has been established that the finite element results do not depend upon the relative size of the unit cell, L/l.

The deformation of a perfect hexagonal honeycomb is governed by cell-wall stretching under hydrostatic loading and by cell-wall bending under deviatoric loading [6]. The difference in deformation mechanisms is reflected in Eq. (5) by the linear dependence of the bulk modulus κ_0 and hydrostatic yield strength σ_H^0 upon the relative density $\bar{\rho}$ and by the non-linear power law dependence of Young's modulus E_0 and uniaxial yield strength σ_U^0 upon $\bar{\rho}$. Consequently, the in-plane hydrostatic yield strength of a perfect honeycomb of relative density $\bar{\rho} = 10\%$ is about an order of magnitude larger than the uniaxial yield strength. On the other hand, experimental studies on commercial metallic foams [2,7,8] all suggest that the hydrostatic yield strength is comparable to the uniaxial strength — the resulting yield surface, when projected onto mean stress versus Mises effective stress space, is nearly circular. It is demonstrated by Chen et al. [1] that this knock-down in hydrostatic strength is associated with bending of the cell walls in the presence of various geometrical imperfections. Furthermore, it is found that the predicted yield surface shape of an initially perfect honeycomb with 5% of its cell edges randomly broken closely resembles the measured yield surface of commercial metal foams (see for example Refs. [2,8]). Thus, regular honeycombs containing 5% randomly fractured cell walls are chosen in the present investigation in order to study the effect of inclusions and holes on stiffness and strength. For brevity, in our finite element study we shall refer to this microstructure as the imperfect honeycomb.

Reference finite element solutions are presented in Fig. 2 for Young's modulus E_I, bulk modulus κ_I, uniaxial yield strength σ_U^I and hydrostatic yield strength σ_H^I of the imperfect honeycomb as a function of the relative density, $\bar{\rho}$. The elastic moduli are calculated from the first increment of loading, and the yield strengths are defined by the peak values of the stress versus strain curves. As expected, neither the bulk modulus nor the hydrostatic yield strength of the imperfect honeycomb depends linearly upon the relative density. Curve fitting of the numerical

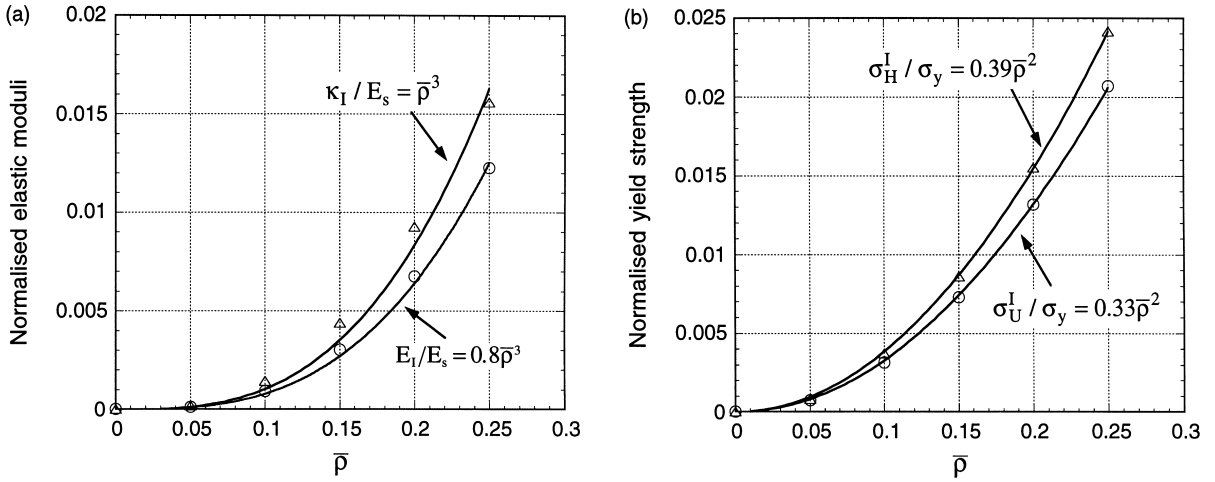

Fig. 2. (a) Elastic moduli and (b) yield strengths of an imperfect honeycomb as functions of relative density $\bar{\rho}$. The open symbols denote finite element results and solid lines are curve fits. The imperfection comprises 5% missing cell walls.

results gives

$$\frac{E_I}{E_s} = 0.8\bar{\rho}^3, \quad \frac{\kappa_I}{E_s} = \bar{\rho}^3,$$
$$\frac{\sigma_U^I}{\sigma_y} = 0.33\bar{\rho}^2, \quad \frac{\sigma_H^I}{\sigma_y} = 0.39\bar{\rho}^2. \tag{7}$$

Expressions (7) adequately describe the numerical results, as seen by a direct comparison in Fig. 2. We shall take Eqs. (7) as the baseline solutions for imperfect honeycombs, in the absence of holes or inclusions. We note in passing that the imperfections lead to a fixed knock-down in uniaxial stiffness and strength by about 40%, independent of relative density. In contrast, the presence of imperfections changes the functional dependence of bulk modulus and hydrostatic strength upon $\bar{\rho}$: the knock-down increases with decreasing $\bar{\rho}$.

3.2. Honeycombs with rigid inclusions or holes

Dimensional analysis of the problem shown in Fig. 1b suggests that the elastic moduli and yield strengths of imperfect honeycombs containing either rigid inclusions or holes can be expressed as

$$\frac{E}{E_M} = f_E(\bar{\rho}, c, D/l), \quad \frac{\kappa}{\kappa_M} = f_\kappa(\bar{\rho}, c, D/l),$$
$$\frac{\sigma_U}{\sigma_U^M} = f_U(\bar{\rho}, c, D/l), \quad \frac{\sigma_H}{\sigma_H^M} = f_H(\bar{\rho}, c, D/l), \tag{8}$$

where the subscript (or superscript) 'M' should be replaced by '0' for a perfect honeycomb and by 'I' for an imperfect honeycomb; E, κ, σ_U and σ_H are the Young's modulus, bulk modulus, uniaxial

yield strength and hydrostatic yield strength of a honeycomb containing either rigid inclusions or holes. The non-dimensional functions f_E, f_κ, f_U and f_H remain to be determined, and the three non-dimensional parameters $\bar{\rho}, c$ and D/l represent the relative density of the honeycomb, the volume fraction of inclusions or holes, and the size of the inclusions or holes relative to the cell size.

For the case of a perfect honeycomb, the properties in the absence of an inclusion or hole are given by Eq. (5), whereas for an imperfect honeycomb the base-line properties are given by Eq. (7). The size effect of inclusions or holes is studied by varying D/l at fixed values of c and $\bar{\rho}$. In an extensive finite element study, we varied the relative size D/l of holes and inclusions in the range of 3–50, for both perfect and imperfect honeycombs having a relative density $\bar{\rho}$ in the range of 0.05–0.25, and c in the range of 0.03–0.09. For perfect and imperfect honeycombs with rigid inclusions and for imperfect honeycombs with holes, we found that the effect of the size ratio D/l on the stiffness and strength of both perfect and imperfect honeycombs is less than 2% and can be neglected. For perfect honeycombs with holes, however, we found that the uniaxial and hydrostatic stiffness and strength decrease as D/l increases, plateauing as $D/l \to \infty$; the variations are less than 5% when D/l exceeds 20, as shown in Fig. 3 for the case $c = 8\%$ and $\bar{\rho} = 5\%$. Furthermore, it is seen from Fig. 3 that the size effect is more pronounced for strength than for stiffness. For simplicity, all subsequent calculations are performed for a fixed relative hole or inclusion size of $D/l = 25$. Consequently, the functional dependence of stiffness and strength upon the microstructural parameters simplifies to

$$\frac{E}{E_M} = f_E(\bar{\rho}, c), \quad \frac{\kappa}{\kappa_M} = f_\kappa(\bar{\rho}, c),$$

$$\frac{\sigma_U}{\sigma_U^M} = f_U(\bar{\rho}, c), \quad \frac{\sigma_H}{\sigma_H^M} = f_H(\bar{\rho}, c), \tag{9}$$

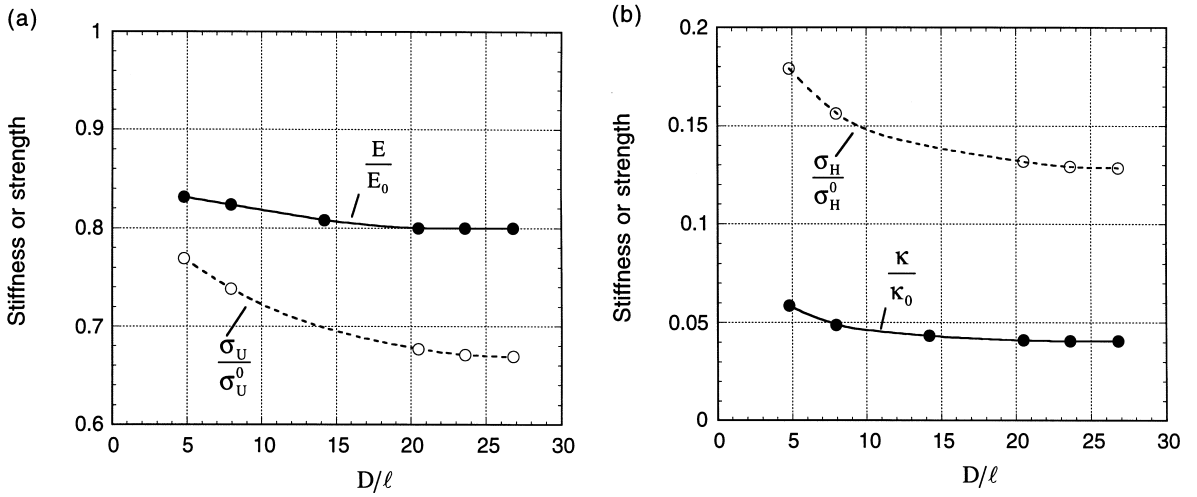

Fig. 3. Dependence of stiffness and strength of perfect honeycombs containing holes on size ratio D/l at $c = 8\%$ and $\bar{\rho} = 5\%$: (a) uniaxial stiffness and strength and (b) hydrostatic stiffness and strength. The hole diameter is designated by D, and l is the cell-wall length.

where 'M' = '0' for an initially perfect honeycomb and 'M' = 'I' for an initially imperfect honeycomb. Finally, we note that the slight elevation in stiffness and strength as shown in Fig. 3 for small values of D/l suggests that a higher-order theory may be more appropriate (see, for example, Refs. [9–12]).

The stress versus strain responses are shown in Fig. 4 for representative cases of uniaxial and hydrostatic stressing of honeycombs without an inclusion or hole, honeycombs with a rigid inclusion ($c = 8\%$), and honeycombs with a hole ($c = 8\%$); both perfect and imperfect honeycombs are considered. Here, $\sigma_m = (\sigma_{11} + \sigma_{22})/2$ is the mean stress, and we take the case $\bar{\rho} = 20\%$ and

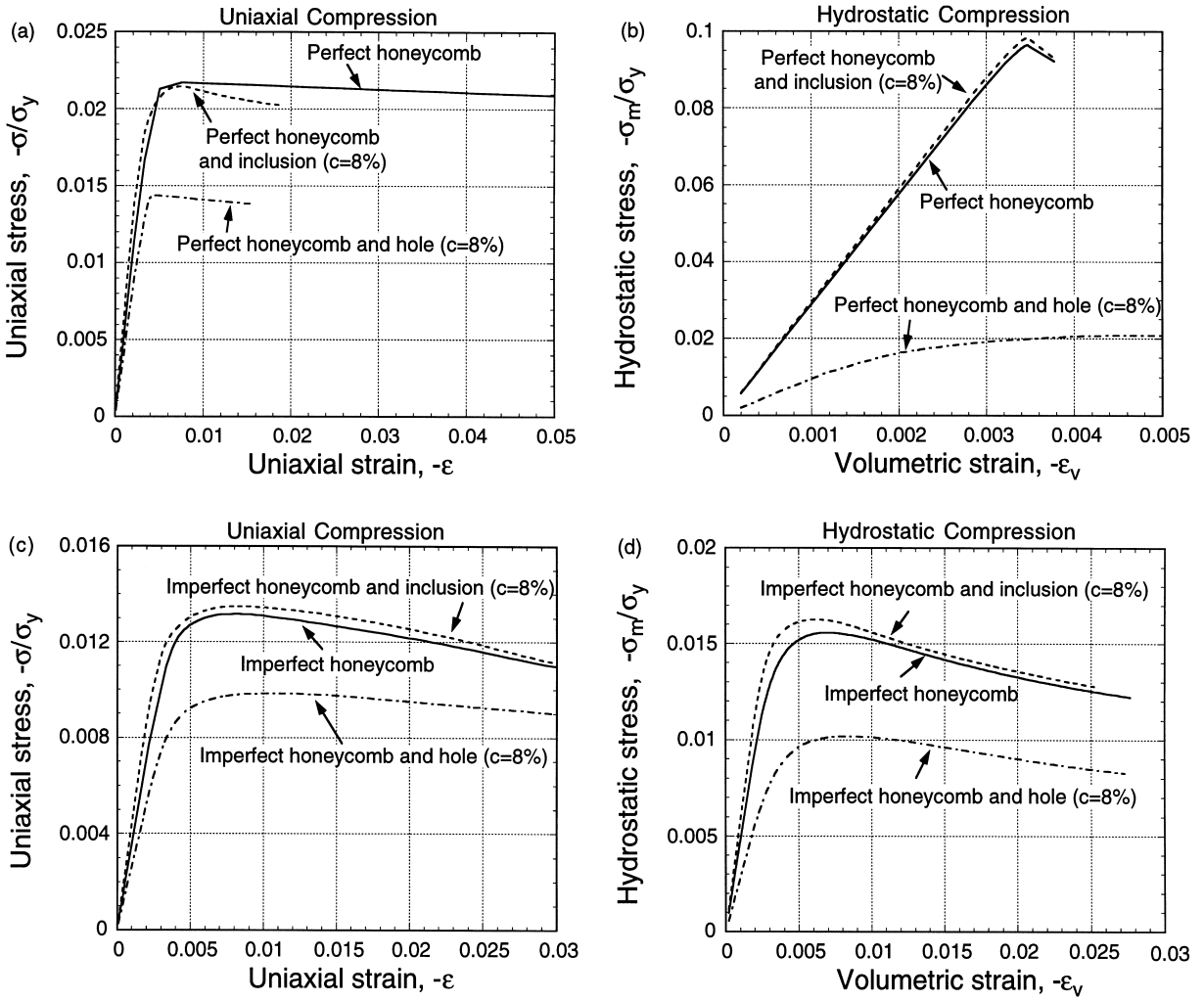

Fig. 4. (a) Uniaxial response of a perfect honeycomb containing inclusions or holes; (b) hydrostatic response of a perfect honeycomb containing inclusions or holes; (c) uniaxial response of an imperfect honeycomb containing inclusions or holes; (d) hydrostatic response of an imperfect honeycomb containing inclusions or holes. The honeycombs are of relative density $\bar{\rho} = 0.2$.

$c = 8\%$ for all honeycombs. Clearly, the sensitivity of the uniaxial and hydrostatic yield strengths (i.e. peak stress) to the presence of a hole is much greater than that of a rigid inclusion for both perfect and imperfect honeycombs. Similar results are obtained for other values of $\bar{\rho}$ and volume fraction c. In fact, it is found that $\sigma_U/\sigma_U^0 = \sigma_H/\sigma_H^0 \cong 1$ for perfect honeycombs and $\sigma_U/\sigma_U^I = \sigma_H/\sigma_H^I \cong 1$ for imperfect honeycombs containing a rigid inclusion, with $\bar{\rho} < 0.25$ and $c \leqslant 0.1$. The effect of the concentration c of inclusions on the elastic moduli is presented in Fig. 5 for a perfect honeycomb and in Fig. 6 for an imperfect honeycomb, for selected values of $\bar{\rho}$. Here, the discrete points denote finite element predictions and the solid lines are fitted curves, given by

$$E/E_0 = 1 + 3.2c, \quad \kappa/\kappa_0 = 1 + 1.5c \tag{10a}$$

for perfect honeycombs and

$$E/E_I = 1 + 3.2c, \quad \kappa/\kappa_I = 1 + 0.2c + 29.3c^2 \tag{10b}$$

for imperfect honeycombs. We note that the normalised elastic moduli are nearly independent of the relative density $\bar{\rho}$ in the relevant range $0 < \bar{\rho} < 0.25$ for both perfect and imperfect honeycombs. Thus the moduli relations given in Eq. (8) reduce considerably to the simple expressions given by Eq. (10).

The influence of holes on the elastic moduli of perfect and imperfect honeycombs is plotted in Figs. 7 and 8, respectively; the corresponding results for yield strengths are shown in Figs. 9 and 10. From Figs. 7a and 9a it is seen that the normalised elastic modulus E/E_0 and the uniaxial yield strength σ_U/σ_U^0 of a perfect honeycomb containing holes depend only on c, and are independent of $\bar{\rho}$. The normalised bulk modulus κ/κ_0 and hydrostatic strength σ_H/σ_H^0 of the perfect honeycomb decrease sharply when a small volume fraction $c \approx 3\%$ of hole is introduced, see Figs. 7b and 9b. A larger volume fraction $c \approx 8.5\%$ induces only a small additional drop in value for κ/κ_0 and σ_H/σ_H^0. A simple interpretation is that the perfect honeycomb without a hole deforms by stretching

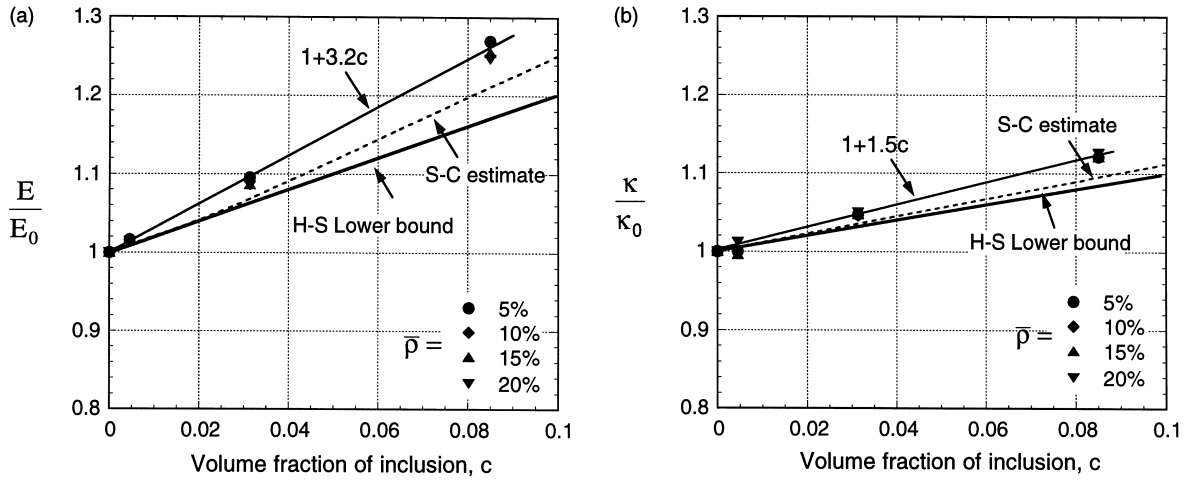

Fig. 5. Effect of volume fraction c of rigid inclusions on (a) Young's modulus and (b) bulk modulus of a perfect honeycomb. The Hashin–Shtrikman (H–S) lower bounds are given by Eq. (18), and the self-consistent (S-C) estimates are given by Eqs. (13) and (24).

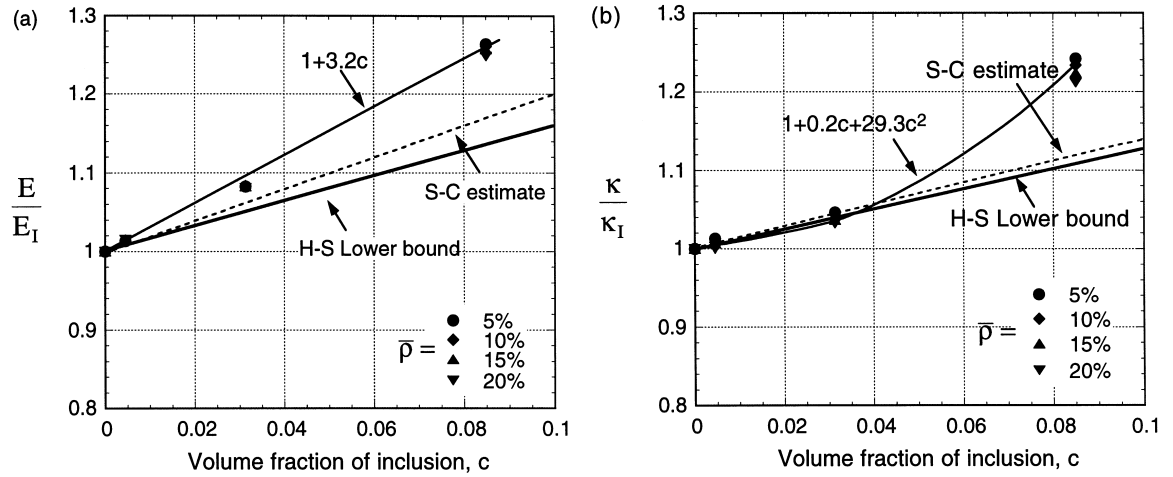

Fig. 6. Effect of volume fraction c of rigid inclusions on (a) Young's modulus and (b) bulk modulus of an imperfect honeycomb. The Hashin–Shtrikman (H–S) lower bounds are given by Eq. (19), and the self-consistent (S-C) estimates are given by Eqs. (13) and (24).

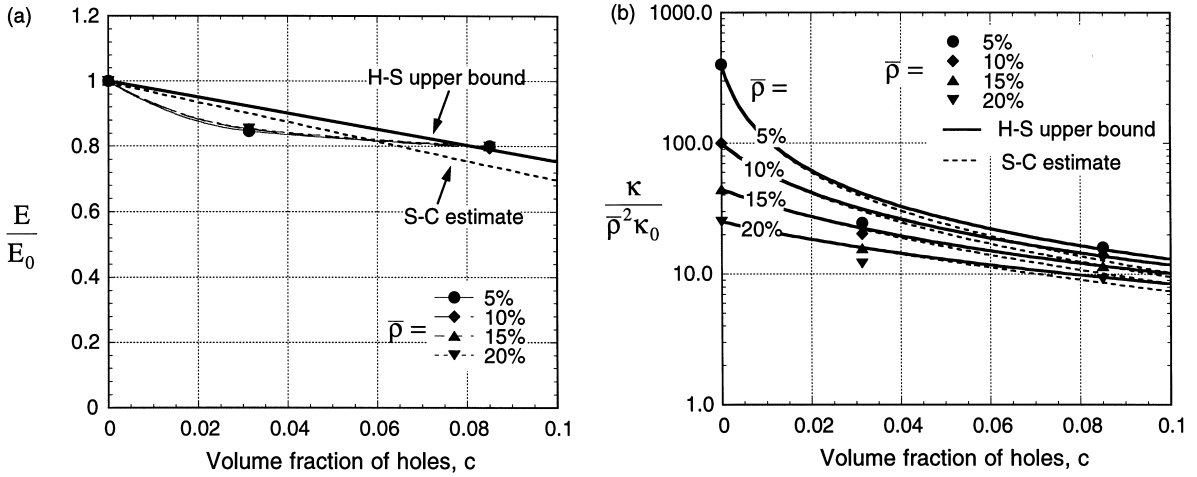

Fig. 7. Effect of volume fraction c of holes on (a) Young's modulus and (b) bulk modulus of a perfect honeycomb. The Hashin–Shtrikman (H–S) upper bounds are given by Eq. (22), and the self-consistent (S-C) estimates are given by Eqs. (25) and (27).

under hydrostatic loading; but the presence of a hole induces deviatoric loading and the response becomes governed by cell-wall bending. On recalling that the bulk modulus of a perfect honeycomb scales with $\bar{\rho}$, whereas that of an imperfect honeycomb scales with $\bar{\rho}^3$, we are led to the choice $\kappa/(\bar{\rho}^2\kappa_0)$ for the appropriate choice of normalised bulk modulus in Fig. 7b. With this choice we find that $\kappa/(\bar{\rho}^2\kappa_0) = 10$–$20$ for the perfect honeycomb containing a hole, for c and $\bar{\rho}$ in the range $3\% \leqslant c \leqslant 8.5\%$ and $5\% \leqslant \bar{\rho} \leqslant 20\%$. At a fixed value of c, the normalised bulk modulus $\kappa/(\bar{\rho}^2\kappa_0)$

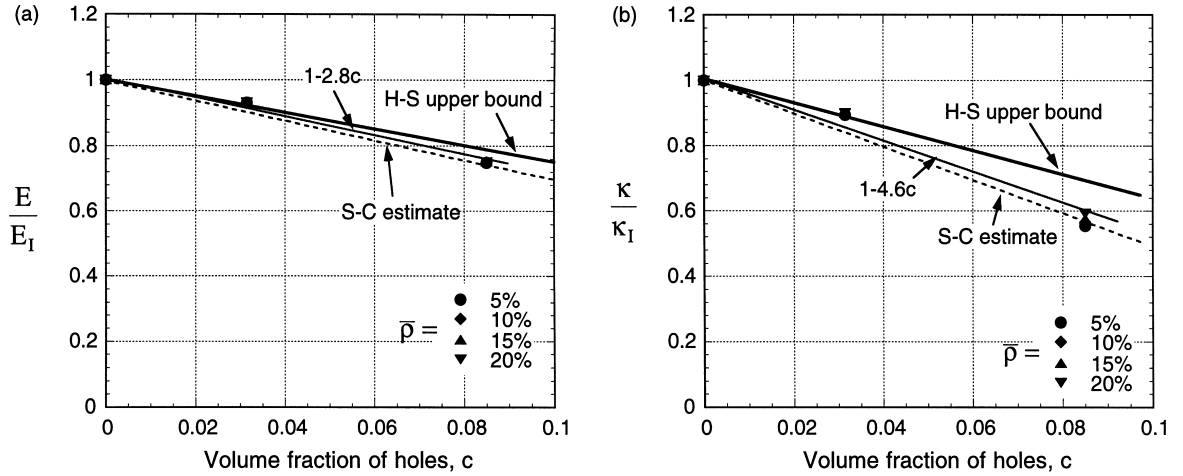

Fig. 8. Effect of volume fraction c of holes on (a) Young's modulus and (b) bulk modulus of an imperfect honeycomb. The Hashin–Shtrikman (H–S) upper bounds are given by Eq. (23), and the self-consistent (S-C) estimates are given by Eqs. (25) and (28).

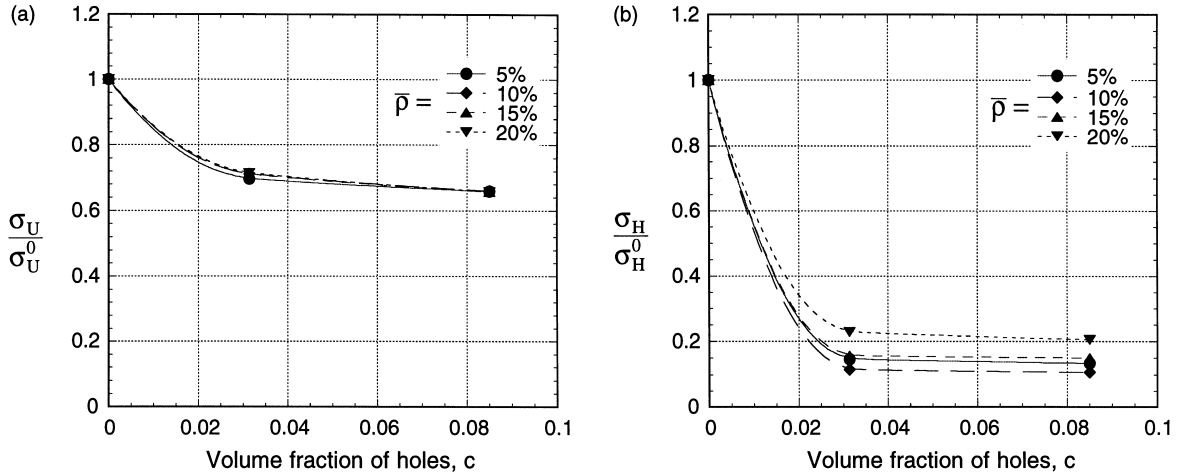

Fig. 9. Dependence of (a) uniaxial yield strength and (b) hydrostatic yield strength on the volume fraction c of holes for a perfect honeycomb.

decreases by a factor of about 2 when $\bar{\rho}$ increases from 5 to 20%. In contrast, κ/κ_0 increases by an order of magnitude when $\bar{\rho}$ increases from 5 to 20%.

Now consider the hydrostatic strength of the perfect honeycomb containing a hole, as displayed in Fig. 9b. If the hole were to induce bending then we would expect the hydrostatic strength to scale with $\bar{\rho}^2$ when a hole is present, and to scale with $\bar{\rho}$ when a hole is absent. Thus it might be expected that a plot of $\sigma_H/(\bar{\rho}\sigma_H^0)$ versus c would show a negligible dependence upon $\bar{\rho}$, at finite value of c. This was not found to be the case, and so the normalised hydrostatic strength in Fig. 9b is displayed

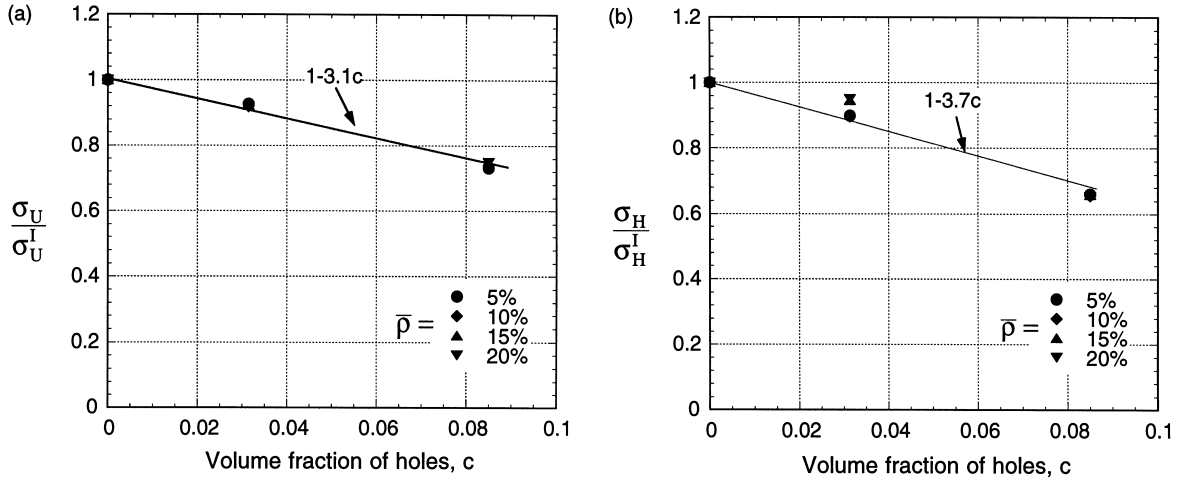

Fig. 10. Dependence of (a) uniaxial yield strength and (b) hydrostatic yield strength on the volume fraction c of holes for an imperfect honeycomb.

as σ_H/σ_H^0. We note that, for $c = 0.03$ and 0.085, the strength σ_H/σ_H^0 increases by a factor of 2 when $\bar{\rho}$ increases by a factor of 4 from 5 to 20%. In fact, σ_H/σ_H^0 shows a greater sensitivity to $\bar{\rho}$ than to the volume fraction c of the hole. The effect of holes on the elasto-plastic properties of imperfect honeycombs is more straightforward: E/E_I, κ/κ_I, σ_U/σ_U^I and σ_H/σ_H^I all decrease as the hole volume fraction c increases, but are independent of $\bar{\rho}$, see Figs. 8 and 10.

3.3. Hashin–Shtrikman bounds of elastic moduli

Perfect and imperfect honeycombs containing rigid inclusions or holes may be treated as two-phase media, with the honeycomb representing the matrix. Under such assumptions, the lower and upper bound estimates for the elastic moduli can be obtained using the approach developed by Hashin and Shtrikman [13]. To accommodate the present problems, a two-dimensional version of the Hashin–Shtrikman bounds for the bulk κ, shear and Young's moduli (i.e. G and E) of an isotropic two-phase medium is derived as

$$\kappa_L = \kappa_1 + \frac{c_2}{[1/(\kappa_2 - \kappa_1)] + c_1/(\kappa_1 + G_1)},$$

$$G_L = G_1 + \frac{c_2}{[1/(G_2 - G_1)] + c_1(\kappa_1 + 2G_1)/[2G_1(\kappa_1 + G_1)]},$$

$$E_L = \frac{4G_L\kappa_L}{G_L + \kappa_L} \tag{11}$$

and

$$\kappa_U = \kappa_2 + \frac{c_1}{[1/(\kappa_1 - \kappa_2)] + c_2/(\kappa_2 + G_2)},$$

$$G_U = G_2 + \frac{c_1}{[1/(G_2 - G_1)] + c_1(\kappa_2 + 2G_2)/[2G_2(\kappa_2 + G_2)]},$$

$$E_U = \frac{4G_U\kappa_U}{G_U + \kappa_U}, \tag{12}$$

where the subscripts 'L' and 'U' denote the lower and upper bounds, the subscripts '1' and '2' refer to quantities associated with phase 1 and 2, respectively, and c_i $(i = 1, 2)$ are the volume fractions of the two phases, with $c_1 + c_2 = 1$. Here and below, it is assumed that phase 2 is stiffer than phase 1. Note that although the bounds for the bulk and shear moduli given by Eqs. (11) and (12) have the same form as those obtained in Refs. [14,15] for the plane-strain bulk modulus and shear modulus of a transversely isotropic composite, the expressions of Young's modulus E in terms of the bulk and shear moduli and κ and G are different:

$$E = 4\kappa G/(\kappa + G) \tag{13}$$

for the present 2D problem whereas

$$E = 3G - (G^2/\kappa) \tag{14}$$

for the plane-strain case.

3.3.1. Rigid inclusions

For a honeycomb/rigid inclusion composite, the Hashin–Shtrikman upper bounds are infinite and hence only the lower bounds are of interest, given by

$$\kappa_L = \kappa_M + \frac{c}{1 - c}(\kappa_M + G_M),$$

$$G_L = G_M + \frac{2cG_M(\kappa_M + G_M)}{(1 - c)(\kappa_M + 2G_M)} \tag{15}$$

and

$$E_L = \frac{4G_L\kappa_L}{\kappa_L + G_L}, \tag{16}$$

where c is the volume fraction of rigid inclusions, and κ_M and G_M are the bulk and shear moduli of the honeycomb matrix. For the perfect honeycomb the subscript 'M' is replaced by '0' and for imperfect honeycomb 'M' is replaced by 'I', following the convention laid down after Eq. (8). For both types of honeycomb, the shear modulus G_M is related to E_M and κ_M by

$$G_M = \frac{E_M\kappa_M}{4\kappa_M - E_M} \tag{17}$$

by manipulation of Eq. (13). For a perfect honeycomb, since $\kappa_0 \gg E_0$ and $\kappa_0 \gg G_0$, Eqs. (13) and (15) for E_L and κ_L simplify to

$$\frac{E_L}{E_0} = 1 + 2c, \quad \frac{\kappa_L}{\kappa_0} = 1 + c \tag{18}$$

for small c. For an imperfect honeycomb $E_I = 0.8\kappa_I$ from Eq. (7) and, for small c, one has

$$\frac{E_L}{E_I} = 1 + \frac{19}{12}c, \quad \frac{\kappa_L}{\kappa_I} = 1 + \frac{5}{4}c. \tag{19}$$

The approximate lower bound solutions (18) and (19) are included in Figs. 5 and 6 (shown as heavy solid lines) for comparison. These bounds lie close to the finite element predictions for $c \leqslant 4\%$ but diverge for larger values of c.

3.3.2. Holes

Hashin–Shtrikman bounds of the elastic moduli can similarly be deduced for a honeycomb/hole composite. Here, only the upper bounds are of physical significance, given by

$$\frac{\kappa_U}{\kappa_M} = \frac{(1-c)G_M}{G_M + c\kappa_M},$$
$$\frac{G_U}{G_M} = \frac{(1-c)\kappa_M}{2cG_M + (1+c)\kappa_M} \tag{20}$$

and

$$E_U = \frac{4G_U\kappa_U}{\kappa_U + G_U}, \tag{21}$$

where c is the volume fraction of holes, and κ_U, G_U and E_U are the upper bounds for the bulk, shear and Young's moduli of the composite. Analogous to the honeycomb-inclusion problem, Eqs. (20) and (21) for E_U and κ_U in the case of a perfect honeycomb matrix can be simplified further to

$$\frac{E_U}{E_0} = \frac{1-c}{1+2c}, \quad \frac{\kappa_U}{\bar{\rho}^2\kappa_0} = \frac{1-c}{\bar{\rho}^2 + 2c/3} \tag{22}$$

upon making use of the result $E_0 \ll \kappa_0$. For the imperfect honeycombs we have $E_I = 0.8\kappa_I$ by Eq. (7), and Eqs. (20) and (21) reduce to

$$\frac{E_U}{E_I} = \frac{1-c}{1+2c}, \quad \frac{\kappa_U}{\kappa_I} = \frac{1-c}{1+4c}. \tag{23}$$

Eqs. (22) and (23) are compared with the finite element predictions in Figs. 7 and 8. As expected, the upper bounds capture the overall trend of decreasing stiffness with increasing volume fraction c of holes, and are in satisfactory agreement with the numerical estimates for the range of c explored.

3.4. Self-consistent estimates of elastic moduli

When the perfect (or imperfect) honeycomb matrix surrounding rigid inclusions (or holes) is approximated by a homogeneous continuum medium, the elastic moduli of the unit cell can be estimated by the self-consistent method. For a honeycomb containing rigid inclusions, a self-consistent calculation for the bulk and shear moduli can be derived from the Eshelby tensor [16] as

$$\frac{\kappa_{sc}}{\kappa_M} = \frac{1}{1 - 2c/(1+\nu_{sc})}, \quad \frac{G_{sc}}{G_M} = \frac{1}{1 - 4c/(3-\nu_{sc})}, \tag{24}$$

where $v_{sc} = (\kappa_{sc} - G_{sc})/(\kappa_{sc} + G_{sc})$, the subscript *sc* denotes the self-consistent estimate, and the subscript '*M*' is replaced by '0' for a perfect honeycomb and '*I*' for an imperfect honeycomb. The bulk and shear moduli κ_{sc} and G_{sc} are obtained by solving the two simultaneous equations (24); the corresponding Young's modulus is given by $E_{sc} = 4\kappa_{sc}G_{sc}/(\kappa_{sc} + G_{sc})$ from Eq. (13). Selected calculations reveal that, in the case of a perfect honeycomb matrix, κ_{sc}/κ_0 and E_{sc}/E_0 are nearly independent of the relative density $\bar{\rho}$ (assuming that $5\% \leqslant \bar{\rho} \leqslant 20\%$), whilst those for the imperfect honeycomb case are strictly independent of $\bar{\rho}$.

The 2D self-consistent estimates of Young's modulus and Poisson's ratio for an isotropic material containing circular holes are [17]

$$\frac{E_{sc}}{E_M} = 1 - 3c, \quad \frac{v_{sc}}{v_M} = 1 - 3c + \frac{c}{v_M} \tag{25}$$

which, in conjunction with $\kappa = E/[2(I - v)]$, give

$$\frac{\kappa_{sc}}{\kappa_M} = \frac{1 - 3c}{1 - 2c + c(4\kappa_M/E_M - 1)}. \tag{26}$$

Here, the subscript M is replaced by '0' for a perfect honeycomb and '*I*' for an imperfect honeycomb. In view of Eq. (5), relation (26) for a perfect honeycomb matrix can be further simplified to

$$\frac{\kappa_{sc}}{\bar{\rho}^2\kappa_0} = \frac{1 - 3c}{\bar{\rho}^2(1 - 3c) + 2c/3} \tag{27}$$

and, by making use of Eq. (7) for an imperfect honeycomb matrix, we obtain

$$\frac{\kappa_{sc}}{\kappa_I} = \frac{1 - 3c}{1 + 2c}. \tag{28}$$

The self-consistent estimates of Young's modulus and bulk modulus are included in Figs. 5–8 as broken lines in order to compare with the finite element results and Hashin–Shtrikman bounds. It is seen that although the elastic moduli calculated by the self-consistent technique are consistently smaller than the Hashin–Shtrikman upper bounds for honeycombs with holes, and larger than Hashin–Shtrikman lower bounds for honeycombs with inclusions, the difference between the self-consistent estimates and the bounds is small (less than 5%).

4. Discussion

4.1. Rigid inclusions

The finite element predictions presented in Figs. 5 and 6 indicate that redundancy defects in the form of rigid inclusions have only a small stiffening effect on the elastic moduli, and a negligible effect on the uniaxial and hydrostatic yield strengths of a honeycomb, be it initially perfect or imperfect. This can be explained as follows. For a perfect honeycomb, the governing deformation mechanisms of cell-wall stretching in the case of hydrostatic pressure and cell-wall bending in the case of uniaxial stressing are not altered by the presence of rigid inclusions. The deformation of an

imperfect honeycomb is governed by cell-wall bending under all stress states, with or without the presence of rigid inclusions. The size effect (D/l) of rigid inclusions is small. Rigid inclusions are considered to be a detrimental type of defect as they increase the mass of the honeycomb for the practical values of $\bar{\rho} < 0.3$: the specific stiffness and specific strength drop due to the presence of rigid inclusions. The elimination of such redundancy inclusions in commercial metallic foams offers a processing opportunity in order to improve the specific properties.

4.2. Holes

The presence of vacancy defects in the form of holes within an initially perfect or imperfect honeycomb has a large influence on both its stiffness and strength, as is evident from Figs. 4 and 7–10. The presence of holes induces bending in cell walls and concentrates deformation near the holes under all macroscopic stress states. For an initially perfect honeycomb under hydrostatic loading, this results in a substantial knock-down of the bulk modulus and hydrostatic strength — the situation is complicated further by the fact that the degree of knock-down depends upon the relative density $\bar{\rho}$ of the honeycomb in addition to the volume fraction c of holes. The upper bound solution (22) and the self-consistent estimate (27) for the normalised bulk modulus depend upon $\bar{\rho}$ as well as upon the hole volume fraction c, consistent with the finite element results shown in Figs. 7b and 9b.

The normalised elastic moduli and yield strengths of the imperfect honeycomb are functions of the volume fraction c of holes only (Figs. 8 and 10), given by the curve-fitting formulas

$$\frac{E}{E_I} = 1 - 2.8c, \quad \frac{\kappa}{\kappa_I} = 1 - 4.6c,$$

$$\frac{\sigma_U}{\sigma_U^I} = 1 - 3.1c, \quad \frac{\sigma_H}{\sigma_H^I} = 1 - 3.7c. \tag{29}$$

Expressions for the moduli close to those given by Eq. (29) can be derived by assuming that the main effect of the holes is to reduce the overall relative density of the unit cell, as follows.

In the absence of holes, the elastic moduli of an imperfect honeycomb are proportional to $\bar{\rho}^3$. The presence of holes leads to a reduction of the relative density of the unit cell from $\bar{\rho}$ to $(1 - c)\bar{\rho}$. If we assume that the effect of holes is only to reduce the average relative density of the unit cell, and assume that Eq. (7) remains valid, then for small c we have

$$\frac{E}{E_I} = 1 - 3c, \quad \frac{\kappa}{\kappa_I} = 1 - 3c. \tag{30}$$

These expressions agree closely with Eq. (29) determined from the finite element calculations. Thus, the uniaxial and hydrostatic stiffness of an imperfect honeycomb is relatively insensitive to the presence of holes when these properties are correlated in terms of the overall relative density of the unit cell.

In order to explore the dependence of strength upon the ligament size between neighbouring holes, the results of Figs. 9 and 10 are replotted in terms of strength versus the D/L ratio, as shown in Fig. 11. Here, the finite element results for perfect and imperfect honeycombs are denoted by solid and open symbols, respectively; the notch-insensitive straight lines denote that the net section

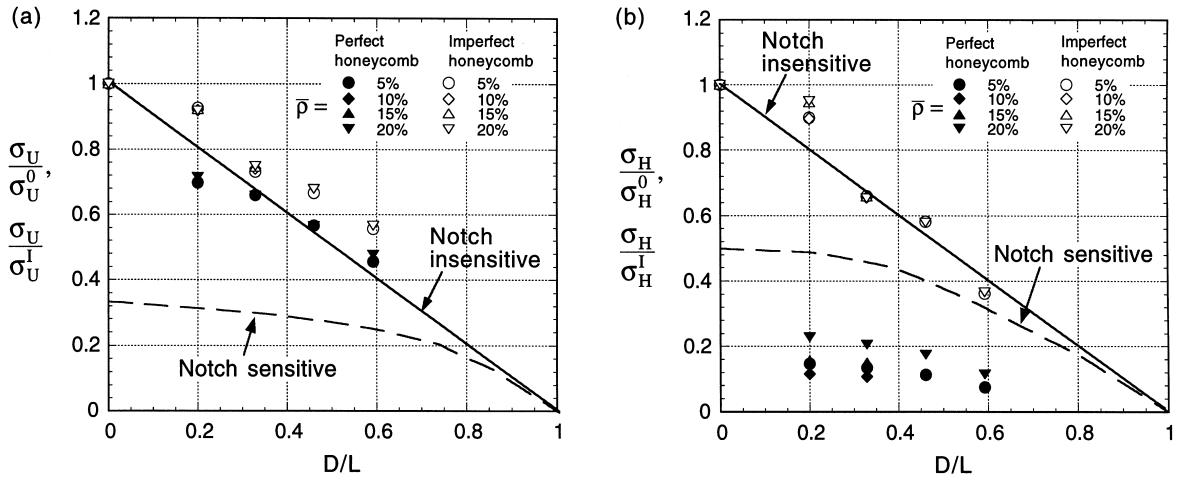

Fig. 11. Dependence of (a) uniaxial yield strength and (b) hydrostatic yield strength on relative hole size D/L for both initially perfect and imperfect honeycombs.

strength criteria $\sigma_U/\sigma_U^M = 1 - D/L$ and $\sigma_H/\sigma_H^M = 1 - D/L$ apply, whilst the notch-sensitive curves represent the inverse of the stress concentration factor of a homogeneous isotropic material due to the introduction of an open hole [18]. Fig. 11 reveals that the uniaxial tensile strength of both perfect and imperfect honeycombs and the hydrostatic strength of imperfect honeycombs comply with the net section strength criterion, consistent with recent experimental measurements on several commercially available metal foams such as Alporas and Cymat [19]. However, a perfect honeycomb subjected to hydrostatic loading exhibits an extreme form of notch-sensitive behaviour, which is due to the fact that under hydrostatic loading the deformation mechanism of a perfect honeycomb is switched from cell-wall stretching to cell-wall bending by the presence of the hole.

5. Conclusions

The sensitivity of the stiffness and strength of honeycombs to the presence of inclusions and holes is analysed using the finite element method. For both perfect and imperfect honeycombs, rigid inclusions have only a small effect on the stiffness and strength. We conclude that the main effect of rigid inclusions in honeycombs is to increase mass, and thereby reduce the specific properties.

For initially perfect honeycombs, the presence of holes causes a substantial knock-down in the bulk modulus and hydrostatic yield strength due to induced cell-wall bending. The stiffness and strength are dependent upon both the volume fraction of holes and upon the relative density of the honeycomb; additionally, a hole size effect is noted when the hole diameter is of the same order of magnitude as the cell size. For imperfect honeycombs containing a small number fraction of randomly broken cell walls, the knock-down in stiffness due to the presence of holes can be

estimated by assuming that the main effect of the holes is to reduce the overall relative density of the honeycomb. The knock-down in strength is consistent with a net section strength criterion.

Both Hashin–Shtrikman bounds and self-consistent estimates describe closely the elastic moduli of perfect and imperfect honeycombs containing either rigid inclusions or holes. These results can be used to guide the processing of commercial foams with improved properties, and to estimate the residual stiffness and strength of as-received foams containing open holes or redundancy inclusions.

Acknowledgements

This work was supported by EPSRC and by the DARPA/ONR MURI program on Ultralight Metal Structures (No. N00014-1-96-1028). The authors are grateful for helpful discussions with Prof. M.F. Ashby.

References

[1] Chen C, Lu TJ, Fleck NA. Effect of imperfections on the yielding of two-dimensional foams. Journal of the Mechanics and Physics of Solids 1999;47:2235–72.
[2] Deshpande VS, Fleck NA. Isotropic constitutive models for metallic foams. Journal of the Mechanics and Physics of Solids 2000, in press.
[3] Guo XE, Gibson LJ. Behaviour of intact and damaged honeycombs: a finite element study. International Journal of Mechanical Sciences 1999;41:85–105.
[4] Silva MJ, Gibson LJ. The effect of non-periodic microstructures and defects on the elastic properties of two-dimensional cellular solids. International Journal of Mechanical Sciences 1995;37:1161–77.
[5] Warren WE, Kraynik AM. Foam mechanics: the linear elastic response of two-dimensional spatially periodic cellular materials. Mechanics of Materials 1987;6:27–37.
[6] Gibson LJ, Ashby MF. Cellular solids: structure and properties, 2nd ed.. Cambridge: Cambridge University Press, 1997.
[7] Zhang J, Lin Z, Wong A, Kikuchi N, Li VC, Yee AF, Nusholts GS. Constitutive modeling and material characterisation of polymeric foams. ASME Journal of Engineering Materials and Technology 1997;119:284–91.
[8] Gioux G, McCormack TM, Gibson LJ. Failure of aluminium foams under multiaxial loads. International Journal of Mechanical Sciences 1999, submitted for publicaltion.
[9] Mindlin RD. Effect of couple stresses on stress concentrations. Experimental Mechanics 1963;3:1–7.
[10] Daniel IM. Strain and failure analysis of graphite-epoxy plates with cracks. Experimental Mechanics 1978;18:246–52.
[11] Anderson WB, Lakes RS. Size effects due to Cosserat elasticity and surface damage in closed-cell polymethacrylimide foam. Journal of Materials Science 1994;29:6413–9.
[12] Fleck NA, Hutchinson JW. Strain gradient plasticity. Advances in Applied Mechanics 1997;33:295–362.
[13] Hashin Z, Shtrikman S. A variational approach to the theory of the elastic behaviour of multiphase materials. Journal of Mechanics and Physics of Solids 1963;11:127–40.
[14] Hill R. Theory of mechanical properties of fibre-strengthened materials — I. Elastic behaviour. Journal of Mechanics and Physics of Solids 1964;12:199–212.
[15] Hashin Z. On elastic behaviour of fibre reinforced materials of arbitrary transverse phase geometry. Journal of Mechanics and Physics of Solids 1965;13:119–34.
[16] Mura T. Micromechanics of defects in solids, 2nd ed. Dordrecht: Martinus Nijhoff Publishers, 1987.
[17] Krajcinovic D. Damage mechanics. New York: Elsevier, 1996.
[18] Peterson RE. Stress concentration factors. New York: Wiley, 1974.
[19] Fleck NA, Olurin OB, Ashby MF. Failure of cellular foams with open holes and deep notches. to be submitted.